Optical Magnetoelectric Effect of Patterned Oxide Superlattices with Ferromagnetic Interfaces

N. Kida,[1] H. Yamada,[2] H. Sato,[2] T. Arima,[1,3] M. Kawasaki,[2,4] H. Akoh,[2] and Y. Tokura[1,2,5]

[1]*Spin Superstructure Project (SSS) and Multiferroics Project (MF), ERATO, Japan Science and Technology Agency (JST), c/o National Institute of Advanced Industrial Science and Technology (AIST), AIST Tsukuba Central 4, 1-1-1 Higashi, Tsukuba, Ibaraki 305-8562, Japan*

[2]*Correlated Electron Research Center (CERC), National Institute of Advanced Industrial Science and Technology (AIST), AIST Tsukuba Central 4, 1-1-1 Higashi, Tsukuba, Ibaraki 305-8562, Japan*

[3]*Institute of Multidisciplinary Research for Advanced Materials, Tohoku University, 2-1-1 Katahira, Aoba-ku, Sendai 980-8577, Japan*

[4]*Institute for Materials Research, Tohoku University, 2-1-1 Katahira, Aoba-ku, Sendai 980-8577, Japan*

[5]*Department of Applied Physics, The University of Tokyo, 7-3-1 Hongo, Bunkyo-ku, Tokyo 113-8656, Japan*

(Received 9 January 2007; revised manuscript received 14 July 2007; published 9 November 2007)

Nonreciprocal directional dichroism, termed the optical magnetoelectric (OME) effect, has been observed in patterned superlattice (SL) composed of perovskite oxides, $LaMnO_3$, $SrMnO_3$, and $LaAlO_3$. Such a tricolor SL with ferromagnetic interfaces is expected to artificially break both space-inversion and time-reversal symmetries and hence to show the OME effect. The Bragg diffraction from the grating structure with a period of 4 μm fabricated on the SL was employed to sensitively detect the OME effect, yielding the relative change of the diffracted light intensity ($\sim$0.2%–0.5%) upon a reversal of either the in-plane magnetization or the propagation vector of the diffracted light.

DOI: 10.1103/PhysRevLett.99.197404 PACS numbers: 78.20.Ls, 42.25.Fx, 75.70.Cn

The magnetoelectric (ME) effect means the induction of the polarization P by a magnetic field H or inversely the induction of the magnetization M by an electric field E [1]. Recently, there is growing interest in realizing the gigantic ME effect, as stimulated by the observation of a magnetic control of the ferroelectric polarization in multiferroic oxides, in which ferroelectricity and magnetism are strongly coupled with each other [1]. Even at an optical frequency ω, the analogous ME effect may show up in materials with lack of both space-inversion and time-reversal symmetries; the electric polarization P^ω can be induced by the light magnetic field H^ω [2–7]. This is referred to as the optical ME (OME) effect. A direct consequence of OME effect is a nonreciprocal directional birefringence or dichroism with respect to the propagation vector k of light. Most prototypically, the nonreciprocity emerges as a change of transmission and reflection [8] when k is set to parallel or antiparallel to the toroidal moment T defined as $P \times M$ [9], which in turn enables us to control the intensity of light by changing the direction of P or M. Up to date, the OME effect has been observed in a variety of bulk materials [2–5,7] with lack of both space-inversion and time-reversal symmetries, besides the chevron shaped permalloy, in which the asymmetric shape of the patterns breaks the space-inversion symmetry [6]. Here we show a new approach to the OME effect with use of unique properties of hetero-epitaxial oxide superlattice (SL); we designed the SL with a stacking sequence of different nonferromagnetic oxides and created the polar ferromagnetism at oxide heterointerfaces, which can intrinsically break both space-inversion and time-reversal symmetries.

The state-of-art pulsed laser deposition (PLD) technique makes it possible to build up different kinds of perovskite oxides in a layer-by-layer manner with coherent epitaxy and to create new electric and magnetic properties at oxide heterointerfaces, which can be neither realized in bulk properties of the constitute oxides nor treated as the simple combination of them [10]. Here we consider ''tricolor'' oxide SL composed of the stacking sequences of three different oxides. This can be viewed as a finite stacking of an asymmetric ''ABC'' structure, where A, B, and C represent different oxides, as schematically shown in Fig. 1(a). Such sequences can artificially break the space-inversion symmetry and are expected to produce the effective electric polarization P_{ABC} in the stacking direction. The presence of such an inherent P_{ABC} has been theoretically considered [11] and identified as an enhancement tool of physical quantities; e.g., dielectric constant [12] and spontaneous polarization [13] in ferroelectric $BaTiO_3/SrTiO_3/CaTiO_3$ SL as well as optical second-harmonic generation (SHG) intensity [14] in $SrTiO_3/LaAlO_3/La_{0.6}Sr_{0.4}MnO_3$ SL.

Recently, the production of the ferromagnetic (FM) state at oxide heterointerfaces has been achieved for the ''bicolor'' SL, composed of two perovskite manganites, $LaMnO_3$ and $SrMnO_3$ [15,16]. Both are antiferromagnetic (AF) insulators in the form of bulk; $LaMnO_3$ has one e_g electron per Mn-site (d^4), while $SrMnO_3$ has no e_g electron (d^3). The spin and orbital ordering patterns of Mn^{3+} ions are depicted in Fig. 1(b) [17]. $LaMnO_3$ is also known as a parent compound of perovskite manganites showing the colossal magnetoresistance (CMR), in which the gigantic change of resistivity is induced by an application of H [17]. A variety of electric phases (e.g., FM phase) acting as a source of CMR effect takes place when the appropriate charge carriers (holes) are doped into $LaMnO_3$ by the substitution of La ions with divalent ions like $La_{1-x}Sr_xMnO_3$. At the artificial $LaMnO_3/SrMnO_3$ interface, the MnO_2

 © 2007 The American Physical Society

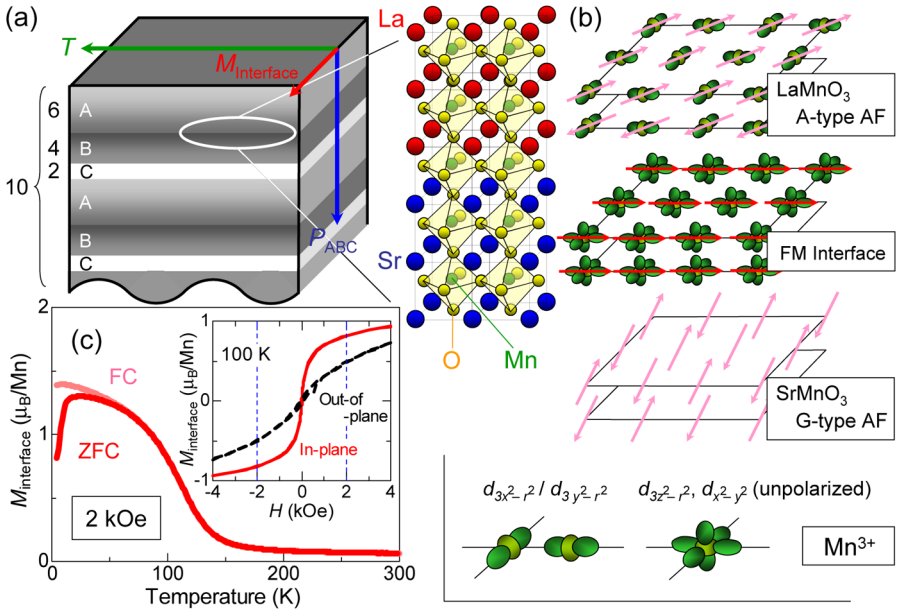

FIG. 1 (color online). (a) Schematic illustration of the atomically controlled tricolor SL. The SL consists of 10 repeated sequences of $LaMnO_3/SrMnO_3/LaAlO_3$ in such a manner as ABCABC..., which can break the space-inversion symmetry along the stacking direction. (b) $LaMnO_3$ and $SrMnO_3$ are *A*-type and *G*-type AF insulators, respectively, while the interface layer is expected to be FM. The anticipated orbital characters at the Mn^{3+}-containing sites are shown schematically. (c) The in-plane magnetization $M_{\text{interface}}$ measured in the field-cooling (FC) and zero field-cooling (ZFC) runs of the SL increase below 150 K in the magnetic field of 2 kOe, indicating the presence of the spontaneous magnetization or equivalently the breaking of the time-reversal symmetry at $LaMnO_3/SrMnO_3$ interfaces. The inset shows the anisotropy of in-plane (solid line) and out-of-plane (dotted line) magnetization measured at 100 K, indicating that the magnetic easy axis lies in the plane. The magnetic fields of ± 2 kOe that we used here are represented by vertical dotted lines.

layer sandwiched by LaO and SrO layers and perhaps the nearby MnO_2 layers as well can be regarded as hole-doped [Fig. 1(a)]. Experimentally, the interface FM state was successfully detected below 200 K [16], indicating the breaking of the time-reversal symmetry at $LaMnO_3/SrMnO_3$ interfaces.

Based on this consideration, we designed tricolor SL composed of $LaMnO_3$, $SrMnO_3$, and $LaAlO_3$ to break the space-inversion symmetry as well and exploited their unique properties at the FM heterointerfaces. We patterned the grating structure on the SL and employed the Bragg diffraction technique in transmission and reflection geometries to enhance and sensitively detect the OME effect.

For the preparation of tricolor $LaMnO_3/SrMnO_3/LaAlO_3$ SL, a PLD method was employed [17]. A (100) surface of the $La_{0.3}Sr_{0.7}Al_{0.65}Ta_{0.35}O_3$ (LSAT) crystal was used as the substrate, whose lattice constant (3.87 Å) nearly matches with those of the SL. The thickness of each $LaMnO_3$, $SrMnO_3$, and $LaAlO_3$ layers was set to 6, 4, and 2 unit cells, respectively. The sequence of $LaMnO_3/SrMnO_3/LaAlO_3$ was repeated 10 times, amounting to the total thickness of 46 nm [Fig. 1(a)]. During the deposition, we monitored the oscillation of the reflection high-energy electron diffraction (RHEED) intensity and confirmed the layer-by-layer growth and the stacking numbers of respective constitute layers. Temperature profile of the in-plane magnetization ($M_{\text{interface}}$ at 2 kOe) of the as-prepared tricolor SL measured by a superconducting quantum interference device (SQUID) magnetometer is displayed in Fig. 1(c), signaling the FM state generated at the interfaces below 150 K. We confirmed that the respective thin films of $LaMnO_3$, $SrMnO_3$, and $LaAlO_3$ as deposited by the similar procedure show essentially no spontaneous magnetization [16].

The direction of $T(= P_{\text{ABC}} \times M_{\text{interface}})$ intrinsically lies within in-plane of SL [Fig. 1(a)], which makes it difficult to detect the OME effect by conventional transmission and reflection experiments. Therefore, we observed the diffracted light intensity from the grating structure, which was patterned on the SL along one of the in-plane axes by a lithography technique [Fig. 2(b)]. In this case, the reciprocal lattice vector *G* of the grating is parallel or antiparallel to *T* [see, Fig. 3(c)], which was proved to be effective to detect the OME effect, experimentally with use of a patterned polar ferrimagnet [18] and also theoretically by the calculation [19]. The grating period and the width of the groove were 4 and 2 μm, respectively. The depth of the groove was carefully set to 50 nm (corresponding to the total thickness of SL) to fully deplete the region of SL. All these were confirmed by the optical [Fig. 2(b)] and the atomic force microscopy images [Fig. 2(c)]. The diffraction due to the grating structure were clearly visible when white light from a light emitting diode was irradiated to the patterned SL [Fig. 2(a)]. We used the Bragg diffraction

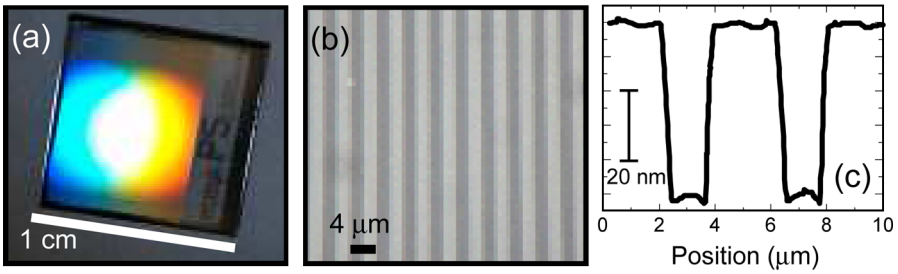

FIG. 2 (color online). (a) Photograph, (b) optical microscopy image, and (c) atomic force microscope profile of the prepared patterned tricolor oxide superlattice.

geometry in Voigt configuration, where the direction of H is perpendicular to the plane of scattering. The configuration of P_{ABC}, $M_{\mathrm{interface}}$, and T is shown in Fig. 3(c). We could observe bright Bragg spots of the order $n = \pm 1$ in transmission and reflection in accord with the diffraction law when the cw light from a laser diode ($\lambda = 785$ nm) was irradiated onto the patterned SL in normal incidence. The light polarization E^{ω} was set along the direction of H to exclude the contribution of the transverse magneto-optical Kerr effect (MOKE). We simultaneously measured the diffracted light intensity I_n for Bragg spots of $n = \pm 1$ in transmission and reflection geometries [Fig. 3(c)] by silicon photodiodes placed within the permalloy cages to prevent the influence of leaking H. The OME effect depends on k_{out}, P_{ABC}, and $M_{\mathrm{interface}}$. Therefore, we measured the relative change ΔI of I_n by a reversal of H, combined with a phase-sensitive detection. Further details of our experimental setup are described elsewhere [18].

First, we present the results of $\Delta I/I_n^{\mathcal{R}}$ of $n = \pm 1$ in the reflection geometry. The signal of $\Delta I/I_{n=\pm 1}^{\mathcal{R}}$ were simultaneously detected during the measurement with sequential reversal of H. Figure 3(a) displays the temperature dependence of $\Delta I/I_{n=1}^{\mathcal{R}}$ (circles) measured by reversals of $H = 2$ kOe. We also measured $\Delta I/I_{n=\pm 1}^{\mathcal{R}}$ at 70 K (and also $\Delta I/I_{n=\pm 1}^{\mathcal{T}}$ in the transmission geometry) with the variation of H between -70 and 70 kOe supplied from a superconducting magnet. However, $I_{n=\pm 1}^{\mathcal{R}}$ ($I_{n=\pm 1}^{\mathcal{T}}$) was found to be dramatically modified up to 5–10% by an application of $H = \pm 70$ kOe. This is assigned to the optical manifestation of the CMR response, which causes the large reconstruction of the electronic structure in the order of eV [17]. Therefore, we used $H = 2$ kOe, which was confirmed to be enough to fully reverse the in-plane $M_{\mathrm{interface}}$ above 50 K on the basis of the in-plane and out-of-plane M-H measurements [Fig. 1(c)], while the contribution of CMR effect remains minimal. As can be seen in Fig. 3(a), the finite $\Delta I/I_{n=1}^{\mathcal{R}}$ in the order of 0.1% appears at low temperatures. With increasing temperature, $\Delta I/I_{n=1}^{\mathcal{R}}$ decreases and tends to vanish rapidly around 100 K. For comparison, the temperature dependence of $M_{\mathrm{interface}}$ is shown for the another piece of the SL sample (not patterned into the grating) by a solid line. The measurement was done in a similar condition, namely, in a warming run with an application of

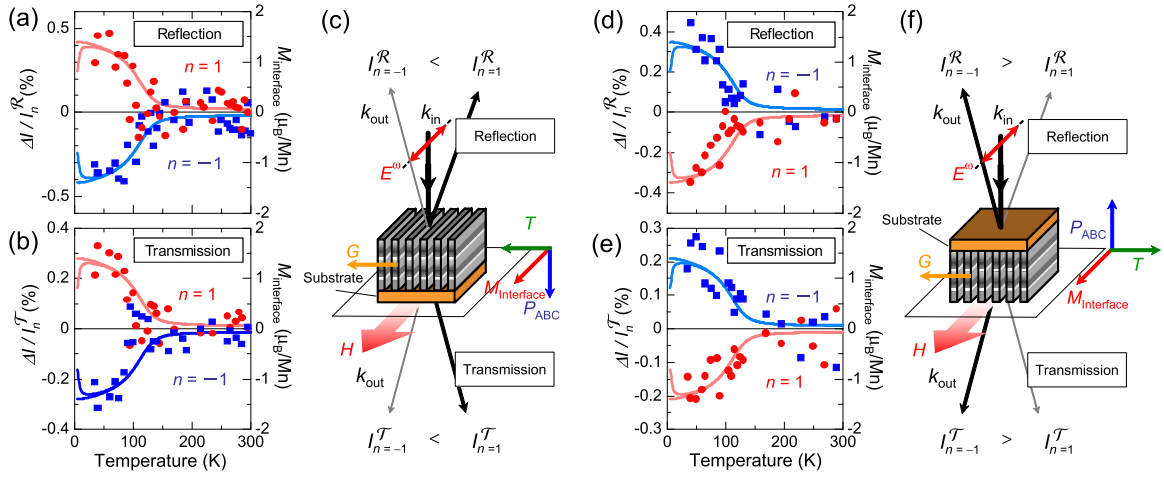

FIG. 3 (color online). The temperature dependence of the relative change of the diffracted light intensity $\Delta I/I_n$ (circles and squares) for Bragg spots of the order $n = \pm 1$ by reversals of the magnetic field H (2 kOe) in (a) reflection and (b) transmission geometries. The temperature dependence of the magnetization $M_{\mathrm{interface}}$ of the tricolor SL is also shown for comparison with solid lines. Solid lines for $n = -1$ are just inversed in sign for clarity of comparison. (c) Schematics of Bragg diffractions from the grating of the tricolor SL in transmission and reflection geometries with the intensities affected by an application of H. The relationships among the directions of the effective electric polarization P_{ABC} induced by asymmetric stacking sequences of different oxides, the interface magnetization $M_{\mathrm{interface}}$ induced at $LaMnO_3/SrMnO_3$ interfaces, and the toroidal moment T defined as $P_{\mathrm{ABC}} \times M_{\mathrm{interface}}$. T is parallel or antiparallel to the reciprocal lattice vector G of the grating. The light polarization E^{ω} is fixed to the direction of H. The temperature dependence of $\Delta I/I_{n=\pm 1}$ in (d) reflection and (e) transmission geometries when the sample was rotated by 180° [(f)].

$H = 2$ kOe. The temperature dependence between $\Delta I/I^{\mathcal{R}}_{n=1}$ and $M_{\text{interface}}$ quite resembles to each other, although the finite $M_{\text{interface}}$ appears above 100 K. This slight discrepancy is ascribed perhaps to the degradation of $M_{\text{interface}}$ during the pattern fabrication process.

A notable feature shown in Fig. 3(a) is the phase reversal when the detector was interchanged from $n = 1$ to $n = -1$, as indicated by squares. In our experimental configuration ($E^{\omega} \parallel H$ and $k_{\text{in}} \parallel P_{\text{ABC}}$), the components of the transverse and longitudinal MOKE are anticipated to be absent, but would become nonzero, if $M_{\text{interface}}$ could not be aligned accurately to the same direction of H due to the possible asymmetry of the grating structures. Nevertheless, the phase of $\Delta I/I^{\mathcal{R}}_{n=-1}$ was found to be changed by π, while the absolute value of $\Delta I/I^{\mathcal{R}}_{n=-1}$ was kept nearly constant. These results clearly indicate that $\Delta I/I^{\mathcal{R}}_{n=\pm 1}$ are affected oppositely with respect to the direction of the in-plane projection of k_{out} as a result of the presence of T [Fig. 3(c)] and hence that $I^{\mathcal{R}}_{n=\pm 1}$ depend on the direction of k. For example, $I^{\mathcal{R}}_{n=1}$ *increases* by an application of H while inversely $I^{\mathcal{R}}_{n=-1}$ *decreases*, as schematically emphasized by a contrast of the trajectory lines of Bragg diffraction [Fig. 3(c)]. Furthermore, the sign of $\Delta I/I^{\mathcal{R}}_{n=\pm 1}$ can be controlled by the reversal of H. This unique characteristic, that is, the nonreciprocal directional dependence of the diffraction, is only expected for the case of the OME effect, not for the conventional MOKE.

The LSAT substrate is conveniently transparent at λ of the laser used here, so that it is possible to make the comparison of the results measured in both transmission and reflection geometries, providing a further insight into the nature of $\Delta I/I_{n=\pm 1}$. Figure 3(b) compare $\Delta I/I^{\mathcal{T}}_{n}$ for $n = 1$ and $n = -1$ measured in the transmission geometry. In accordance with the results of $\Delta I/I^{\mathcal{R}}_{n=\pm 1}$ [Fig. 3(a)], the phase reversal is also discerned and the absolute values of $\Delta I/I^{\mathcal{T}}_{n=\pm 1}$ are comparable to those of $\Delta I/I^{\mathcal{R}}_{n=\pm 1}$, clearly manifesting the OME characteristics. In addition, an important feature is to be noticed in Fig. 3(b); the sign of $\Delta I/I^{\mathcal{T}}_{n=1}$ ($\Delta I/I^{\mathcal{T}}_{n=-1}$) is identical to that of $\Delta I/I^{\mathcal{R}}_{n=1}$ ($\Delta I/I^{\mathcal{T}}_{n=-1}$). This again confirms that $\Delta I/I^{\mathcal{T}}_{n=\pm 1}$ is determined by the direction of T as is characteristic of the OME effect.

To further confirm that the observed signal is odd with respect to P_{ABC}, we also measured $\Delta I/I^{\mathcal{R}}_{n=\pm 1}$ and $\Delta I/I^{\mathcal{T}}_{n=\pm 1}$ while the sample was rotated by 180° around the direction of H, as schematically shown in Fig. 3(f). This operation reverses the direction of P_{ABC}, producing the reversal of T. Indeed, the sign reversal of $\Delta I/I^{\mathcal{R}}_{n=\pm 1}$ and $\Delta I/I^{\mathcal{T}}_{n=\pm 1}$ can be discerned in both geometries, as shown in Figs. 3(d) and 3(e), respectively, although the absolute value is slightly different due to the change of the experimental setup. We also performed the same experiments using a patterned bicolor SL composed of $LaMnO_3$ and $SrMnO_3$ possessing the space-inversion symmetry and to find no detectable signal within the capability of our detection system. The measured magnitude of $\Delta I/I_{n=\pm 1}$ was our detection limit in the order of 0.1% and $\Delta I/I_{n=\pm 1}$ exhibits no systematic sign reversal by changing the detector position from $n = 1$ to $n = -1$. These results ensure that the OME effect comes from the interface, neither the surface of SL nor the asymmetry of the grating structure.

In summary, we have designed and fabricated the tricolor oxide SL composed of $LaMnO_3$, $SrMnO_3$, and $LaAlO_3$ with the anticipation of breaking both space-inversion and time-reversal symmetries. We could demonstrate the OME diffraction signals for this tailor-made noncentrosymmetric SL with even a larger magnitude than those from the bulk materials [2–5,7]. Conversely, we could successfully prove that the interface between the two Mott insulators, $LaMnO_3$ and $SrMnO_3$, is polar and ferromagnetic in nature. The OME effect, arising from the vector product of effective polarization P and magnetization M, sensitively reflects the symmetry breaking at the ferromagnetic state, and hence will be widely applicable to versatile magnetic interface states.

We thank Y. Tokunaga for useful comments. This work was in part supported by Grant-In-Aids for Scientific Research (Nos. 16760035 and 17340104) from the Ministry of Education, Culture, Sports, Science and Technology (MEXT), Japan.

[1] For recent reviews, M. Fiebig, J. Phys. D **38**, R123 (2005); Y. Tokura, Science **312**, 1481 (2006); Y. Tokura, J. Magn. Magn. Mater. **310**, 1145 (2007).
[2] B. B. Krichevtsov *et al.*, J. Phys. Condens. Matter **5**, 8233 (1993); Phys. Rev. Lett. **76**, 4628 (1996).
[3] T. Roth and G. L. J. A. Rikken, Phys. Rev. Lett. **88**, 063001 (2002).
[4] G. L. J. A. Rikken, C. Strohm, and P. Wyder, Phys. Rev. Lett. **89**, 133005 (2002).
[5] J. H. Jung *et al.*, Phys. Rev. Lett. **93**, 037403 (2004).
[6] N. Kida *et al.*, Phys. Rev. Lett. **94**, 077205 (2005).
[7] Y. Shimada *et al.*, Appl. Phys. Lett. **89**, 101112 (2006).
[8] For a recent breviary, L. D. Barron, Nature (London) **405**, 895 (2000).
[9] H. J. Ross, B. S. Sherborne, and G. E. Stedman, J. Phys. B **22**, 459 (1989).
[10] For a recent breviary, H. Y. Hwang, Science **313**, 1895 (2006).
[11] N. Sai, B. Meyer, and D. Vanderbilt, Phys. Rev. Lett. **84**, 5636 (2000).
[12] M. P. Warusawithana, E. V. Colla, J. N. Eckstein, and M. B. Weissman, Phys. Rev. Lett. **90**, 036802 (2003).
[13] H. N. Lee *et al.*, Nature (London) **433**, 395 (2005).
[14] Y. Ogawa *et al.*, Phys. Rev. Lett. **90**, 217403 (2003).
[15] P. A. Salvador *et al.*, Appl. Phys. Lett. **75**, 2638 (1999).
[16] H. Yamada *et al.*, Appl. Phys. Lett. **89**, 052506 (2006).
[17] For a recent review, Y. Tokura, Rep. Prog. Phys. **69**, 797 (2006).
[18] N. Kida *et al.*, Phys. Rev. Lett. **96**, 167202 (2006).
[19] K. Sawada and N. Nagaosa, Appl. Phys. Lett. **87**, 042503 (2005).